Experimental verification of coherent diffractive imaging by a direct phase retrieval method with an aperture-array filter

Experimental verification of coherent diffractive imaging by a direct phase retrieval method with an aperture-array filter

Nobuharu Nakajima

Faculty of Engineering, Shizuoka University, 3-5-1 Johoku, Naka-ku, Hamamatsu, 432-8561, Japan
tsnnaka@ipc.shizuoka.ac.jp

Received Month X, XXXX; revised Month X, XXXX; accepted Month X, XXXX; posted Month X, XXXX (Doc. ID XXXXX); published Month X, XXXX

Recently we have proposed a novel coherent diffractive imaging using a noniterative phase retrieval method with the filter of an aperture array. The first experimental demonstration of this coherent imaging is presented here, in which a complex-valued object illuminated by a laser diode is reconstructed from isolated diffraction intensities of the object's wave field transmitted through an array filter of square apertures by using the phase retrieval method. This imaging method requires only a single measurement of the diffraction intensity and does not need a tight object's support constraint utilized in iterative phase retrieval algorithms or a reference wave used in holographic techniques. © 2010 Optical Society of America

OCIS Codes: 100.0100, 100.5070

Lensless coherent imaging from diffraction intensities, in principle, provides wavelength-limited resolution without the aberration and the finite extent of a lens. In particular, coherent x-ray diffractive imaging has attracted considerable attention during the past decade, because the resolution of x-ray optics such as Fresnel zone plates is many times the wavelength of the x rays. In various approaches to the diffractive imaging, object imaging from a single-shot intensity measurement is especially important, because it enables us to observe an object in real time, and also it allows the reduction of sample damage by an x-ray illumination. Some approaches to such lensless object imaging from a single diffraction intensity measurement have been proposed, for example, in-line [1,2] or off-axis holography [3], interferometric method with a reference illumination containing sharp features [4,5] or a well-characterised illumination [6] or a special designed pinhole array [7], iterative phase retrieval image reconstruction [8,9], combined method of in-line holography and iterative phase retrieval [10], and so forth. In such holographic and interferometric methods, however, the spatial resolution is limited by the range of the Fourier spectrum of a reference wave. On the other hand, the convergence of iterative methods becomes generally difficult in the case of the reconstruction of complex-valued objects, and hence *a priori* information such as tight support constraints or good initial estimates of the objects is necessary.

Recently we have proposed [11] a nonholographic and noniterative phase-retrieval method that allows the reconstruction of a complex-valued object from a single diffraction intensity pattern measured with an aperture-array filter. In this Letter the proof-of-concept experiment of this method is demonstrated at optical wavelengths.

The optical system used in the experiment is shown in Fig.1. A diode laser beam of wavelength $\lambda = 0.635\,\mu$m through a circular pinhole was used to illuminate a negative USAF 1951 resolution target as an object. The strength and polarization of the light was controlled by a polarizer placed in front of the laser. An array filter was placed at a distance of $z = 530\,$mm downstream of the object. The array filter consists of a 64×64 array of square apertures of each width $w = 0.1\,$mm distributed over Cartesian coordinates $(x_n, y_m) = (nd, md)$, (n or $m = -32\cdots, 0, \cdots 31$), of period $d = 0.2\,$mm, which was made by depositing chromium on a glass slide of 1 mm thickness. The plane of the aperture array can be regarded as the Fraunhofer (or Fresnel) diffraction plane for the object's area illuminated through the pinhole of $\sigma = 0.4\,$mm (or 0.6 mm) diameter. The diffraction pattern from the array filter was measured at a distance of $l = 6.8\,$mm using a 1024×1024, 15-bit, 13 μm pixel pitch, Apogee (AP47P) CCD detector.

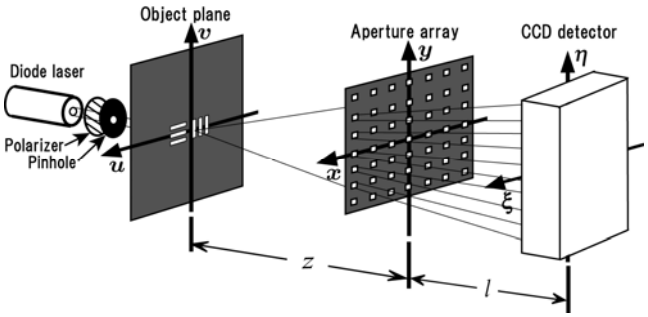

Fig. 1. Schematic arrangement of the experiment. The isolated diffraction intensity of each aperture from those of the adjoining apertures is measured in the detector.

The outline of the method [11] is as follows. When the diffraction pattern of each square aperture in the detector is isolated approximately from those of the adjoining apertures, the measured intensity of the amplitude distribution $K(\xi,\eta)$ at the coordinates $(\xi,\eta) = (ax_n, ay_m)$, (where $a = 1 + l/z$) can be written as

$$\left|K(ax_n, ay_m)\right|^2 \cong \left|\int\int_{-\infty}^{\infty} F(x,y)R(x-x_n, y-y_m)\,dxdy\right|^2, \qquad (1)$$

where $F(x, y)$ is the Fourier (or Fresnel) transform of an object amplitude $f(u, v)$ and $R(x, y)$ is the amplitude transmittance (1.0 within each square and 0.0 otherwise). Since the period d of the array is smaller than $\lambda z/2\sigma$, the intensity pattern of the correlation can be encoded into the discrete data measured in the detector by the sampling theorem. Let $|K(ax_n, ay_m)|$ and $\phi(x_n, y_m)$ be the modulus and the phase, respectively, of $K(ax_n, ay_m)$. Under the Gaussian approximation of the square aperture's function, the one-dimensional (1-D) phases of $\phi(x_n, y_m)$ along lines parallel to the x axis can be calculated from sampling data of $|K(\xi, \eta)|$ at the points of coordinates $(\xi, \eta) = (ax_n \pm \tau, ay_m)$ by [11]

$$\phi(x_n, y_m) \cong \Im^{-1}\left[\frac{\Im[D(x_n, y_m)]}{2i\sinh(2\pi c\alpha)}\right], \qquad (2)$$

where $\Im[\cdots]$ and $\Im^{-1}[\cdots]$ denote the 1-D Fourier and the inverse Fourier transforms, respectively, α is the coordinate in the Fourier space for x_n – coordinate, $D(x_n, y_m) = \ln[|K(ax_n + \tau, ay_m)|/|K(ax_n - \tau, ay_m)|]$, and $c = \pi\tau w^2/(6\lambda l)$, in which τ is a known constant. The 1-D phases along lines parallel to the y axis are also retrieved from sampling data of $|K(\xi, \eta)|$ at the points of coordinates $(\xi, \eta) = (ax_n, ay_m \pm \tau)$. Then the overall two-dimensional phase $\phi(x_n, y_m)$ can be determined by combining those 1-D phases in the directions of x and y axes. Finally, the object $f(u, v)$ can be reconstructed through compensation for the known function $R(x, y)$ from the inverse Fourier transform of the retrieved correlation integral $K(ax_n, ay_m)$ in Eq. (1).

The calculation of the phase was done from only a single diffraction pattern in the detector. No other calibration was performed on the data except that a chosen center of the measured diffraction pattern was shifted to the center of the 1024×1024 sampling points, and that a constant bias component due to the noise of the CCD was subtracted from the measured data. In this system, the lateral resolution of the reconstruction is theoretically limited [11] by λ/NA $(\cong 52.6\mu\mathrm{m})$, where the NA is the numerical aperture of the array filter, defined by $\mathrm{NA} \cong 32d/z\,(\cong 0.0121)$.

Figure 2 shows the first example of the experiments. Figure 2(a) shows the modulus of the object image by a convex lens of focal length 120 mm, which is inserted between the object and the CCD instead of the aperture-array filter. This object corresponds to lines in the portion (group 3, element 4) of the USAF 1951 target illuminated through a circular pinhole of 0.4-mm. The picture of Fig. 2(a) is represented on the same resolution as in the optical system with the array filter.

Figure 2(b) shows the measured intensity through the aperture-array filter without lenses. Figures 2(c) and 2(d) show the modulus and the phase, respectively, of the reconstructed object using the direct phase retrieval with Eq. (2) from multiple groups of sampling data of the intensity distribution in Fig. 2(b), consisting of one group of 64×64 sampling data at the coordinates $(\xi, \eta) = (ax_n, ay_m)$, and twenty groups of 64×64 sampling data at the coordinates $(ax_n \pm \tau, ay_m)$ and $(ax_n, ay_m \pm \tau)$ with five values of τ at intervals of a quarter of the CCD's pixel, which were used to improve

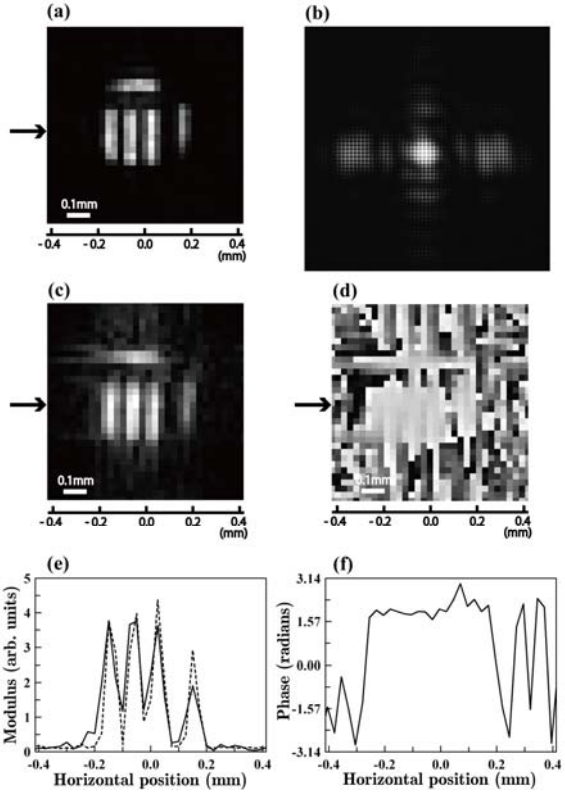

Fig. 2. (a) Modulus of the object image by a convex lens. (b) Measured intensity pattern. (c) Modulus and (d) phase of the reconstructed object. The solid curves in (e) and (f), and the dotted curve in (e) show the cross-sectional profiles of (c) and (d), and (a), respectively, along horizontal lines through the positions indicated by the arrows.

the accuracy of the phase calculation [11]. Since those coordinates did not coincide with the positions of the measured data (1024×1024 points) in Fig. 2(b), the intensity data at those coordinates were calculated only from the measured data by a linear interpolation.

In order to prevent the phase calculation in Eq. (2) from aliasing, the resultant data with 64×64 sampling points were transformed into the data with 256×256 sampling points by using an inverse Fourier transform of the function embedded the Fourier transform of the data 64×64 in the 256×256 points of zero data. Figures 2(c) and 2(d) are shown in the central 33×33 points of the reconstructed object by an inverse Fourier transform of the complex function consisting of the measured modulus and the retrieved phase, where the phase curvature of the illuminating beam was compensated for. In Fig. 2(e), the solid and the dotted curves show the cross-sectional profiles of the moduli of the reconstruction and the image in Figs. 2(c) and 2(a), respectively, along horizontal lines through the positions indicated by the arrows, provided that the total intensity for Fig. 2(c) was matched with that for Fig. 2(a). Figure 2(f) shows the cross-sectional profile of the reconstructed phase shown in Fig. 2 (d) along the same line as in Fig. 2(c). The reconstruction is in good agreement with the modulus image, and the reconstructed phase shows

nearly constant among the images of lines in relation to the original object having no phase variation. The effect of noises on the reconstruction in Fig. 2(c) is larger than that in Fig. 2(a). This reason is that the phase retrieval from the Fourier intensity distribution is influenced by noises on the whole surface of the CCD in contrast to the modulus image containing noises in a small part of the CCD. Note that the three lines (for group 3, element 4 of the USAF 1951 target) with the period ($\cong 88.5\mu$m) is resolved. This fact shows that the resolution of the system is not limited by the aperture's size (0.1mm) of the filter unlike the method with a pinhole array [7].

Figure 3 shows the reconstruction of an object with phase variation. Figure 3(a) shows the modulus image by the same lens as in Fig. 2(a). This object consists of the circular pinhole of 0.6-mm and the lines in the portion (group 2, element 6) of the USAF 1951 target, of which three lines were covered with a film of half-wave retarder as shown in Fig. 3(a). The film has a thickness and index of refraction such that it retards the phase of a light of wavelength $0.560\,\mu$m by π radians relative to the phase retardation of the light in the air. Thus we investigated the retardation of the illuminating light of wavelength $0.635\,\mu$m by using another interferometric experiment. As a result, it was found that the film retards the phase of the illuminating light by about 2.77 radians relative to the retardation in the air. This retardation agrees with the theoretical expectation [i.e., $\pi\times(0.560/0.635)$].

Figure 3(b) shows the measured intensity through the aperture-array filter without lenses. Figures 3(c) and 3(d) show the modulus and the phase, respectively, of the reconstructed object (which are shown in the central 33×33 points of the reconstructed object with 256×256 points) using the same calculation as in Fig. 2 from the intensity in Fig. 3(b). The solid curves in Figs. 3(e) and 3(f), and the dotted curve in Fig. 3(e) show the cross-sectional profiles of the reconstructed modulus and phase in Figs. 3(c) and 3(d), and the modulus image in Figs. 3(a), respectively, along horizontal lines through the positions indicated by the arrows, provided that the total intensity for Fig. 3(c) was matched with that for Fig. 3(a). In Fig. 3(d), the average value and the standard deviation of the phase difference between three lines covered with the film and one line in the air became about 2.79 and 0.19 radians, respectively. It was found that the object's phases in Figs. 2(d) and 3(d) were reconstructed with the accuracy of about $\pm2\pi/30$ radians. On the other hand, the normalized root-mean square errors (i.e., Eq. (21) in [11]) of the reconstructed moduli in Figs. 2(c) and 3(c) were 0.430 and 0.435, respectively, on the basis of each corresponding image.

In conclusion, we have experimentally demonstrated coherent diffractive imaging from a single intensity measurement with the aperture-array filter. Reconstructions of the complex-valued objects have been shown by using the noniterative phase retrieval method without a reference wave. We did not make use of the tight object's support constraint needed in the iterative methods [8,9]. The resolution of the present system is limited not by the aperture's size of the array filter but by the numerical aperture of the array filter. Therefore, there is a possibility that the present method provides a useful means of coherent x-ray diffractive imaging with wavelength resolution.

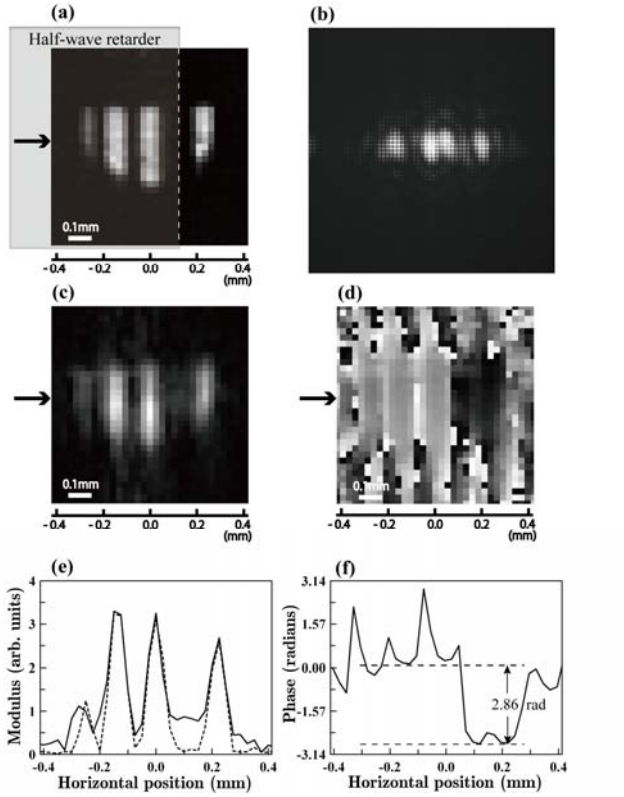

Fig. 3. Same as Fig. 2, except for the object with phase variation. The three lines of the object were covered with a film of half-wave retarder.

References

1. Morlens, J. Gautier, G. Rey, P. Zeitoun, J. Caumes, M. Kos-Rosset, H. Merdji, S. Kazamias, K. Cassou, and M. Fajardo, Opt. Lett. **31**, 3095-3097 (2006).
2. A. Rosenhahn, R. Barth, F. Staier, T. Simpson, S. Mittler, S. Eisebitt, and M. Grunze, J. Opt. Soc. Am. A **25**, 416-422 (2008).
3. S. Eisebitt, J. Lüning , W. F. Schlotter, M. Lörgen , O. Hellwig, W. Eberhardt, and J. Stöhr , Nature **432**, 885-888 (2004).
4. S. G. Podorov, K. M. Pavlov, and D. M. Paganin, Opt. Express **15**, 9954-9962 (2007).
5. D. Zhu, M. Guizar-Sicairos, B. Wu, A. Scherz, Y. Acremann, T. Tylisztzak, P. Fischer, N. Friedenberger, K. Ollefs, M. Farle, J. R. Fienup and J. Stöhr , Phys. Rev. Lett., **105**, 043901 (2010).
6. A. V. Martin and L. J. Allen, Opt. Commun. **281** (2008) 5114-5121.
7. C. S. Guo, K. Liang, X. T. Zhang, and H. T. Wang, Opt. Lett. **35**, 850-853 (2010).
8. J. R. Fienup, Appl. Opt. **21**, 2758-2769 (1982).
9. H. N. Chapman, A. Barty, S. Marchesini, A. Noy, S. P. Hau-Riege, C. Cui, M. R. Howells, R. Rosen, H. He, J. C. H. Spence, U. Weierstall, T. Beetz, C. Jacobsen, and D. Shapiro, J. Opt. Soc. Am. A **23**, 1179-1200 (2006).
10. B. Abbey, K. A. Nugent, G. J. Williams, J. N. Clark, A. G. Peele, M. A. Pfeifer, M. De Jonge and I. McNulty, Nat. Phys., **4**, 394-398 (2008).
11. N. Nakajima, J. Opt. Soc. Am. A **25**, 742-750 (2008).